Neurobiology of Aging 84 (2019) 131–140

Contents lists available at ScienceDirect

Neurobiology of Aging

journal homepage: www.elsevier.com/locate/neuaging

Retrograde axonal transport of BDNF and proNGF diminishes with age in basal forebrain cholinergic neurons

Arman Shekari, Margaret Fahnestock*

Department of Psychiatry and Behavioural Neurosciences, McMaster University, Hamilton, Ontario, Canada

ARTICLE INFO

Article history:
Received 25 March 2019
Received in revised form 22 July 2019
Accepted 31 July 2019
Available online 10 August 2019

Keywords:
Axonal transport
Neurotrophins
Neurodegeneration
Basal forebrain
Alzheimer's disease
Trk receptors

ABSTRACT

Basal forebrain cholinergic neurons (BFCNs) are critical for learning and memory and degenerate early in Alzheimer's disease (AD). BFCNs depend for their survival and function on nerve growth factor (NGF) and brain-derived neurotrophic factor (BDNF), which are retrogradely transported from BFCN targets. Age is the greatest risk factor for developing AD, yet the influence of age on BFCN axonal transport is poorly understood. To model aging, embryonic rat basal forebrain or cortical neurons were cultured in microfluidic chambers. Senescence-associated beta-galactosidase staining indicated an aging phenotype only in BFCNs cultured for 18+ days in vitro. BDNF axonal transport impairments were observed exclusivley in aged BFCNs. BFCNs displayed robust proNGF transport, which also diminished with in vitro age. The expression of NGF receptor tropomyosin-related kinase-A and BDNF receptor tropomyosin-related kinase-B also decreased significantly with in vitro age in BFCNs only. These results suggest a unique vulnerability of BFCNs to age-induced transport deficits. These deficits, coupled with the reliance of BFCNs on neurotrophin transport, may explain their vulnerability to age-related neurodegenerative disorders like AD.

© 2019 Elsevier Inc. All rights reserved.

1. Introduction

The basal forebrain is the primary source of cholinergic innervation in the central nervous system (CNS) and plays a critical role in learning, memory, attention, and regulation of cortical blood flow (Ballinger et al., 2016; Baxter and Chiba, 1999; Linville and Arnerić, 1991). Diffuse projections from basal forebrain cholinergic neurons (BFCNs) terminate mainly in the hippocampus and throughout the cortex (Ballinger et al., 2016). These projections, especially those of the septohippocampal tract, have been shown to degenerate with age (Grothe et al., 2012; Ypsilanti et al., 2008). Degeneration of the basal forebrain has been repeatedly observed in age-related neurodegenerative disorders like Alzheimer's disease (AD), with multiple studies demonstrating that basal forebrain dysfunction is predictive of the disorder (Baker-Nigh et al., 2015; Ballinger et al., 2016; Schmitz et al., 2016; Teipel et al., 2014). Furthermore, synaptic loss in BFCNs correlates strongly with dementia severity in AD and is implicated in aging and age-associated memory deficits (Ballinger et al., 2016; Ferreira-Vieira et al., 2016; Whitehouse et al., 1982; Ypsilanti et al., 2008).

Age-related degeneration of BFCNs may occur because of their unique reliance on target-derived trophic support. BFCNs do not make their own neurotrophins. They rely on their cortical and hippocampal targets to produce brain-derived neurotrophic factor (BDNF) and nerve growth factor (NGF) that are transported back to BFCN cell bodies via retrograde axonal transport (DiStefano et al., 1992; Götz et al., 2001; Seiler and Schwab, 1984; Sobreviela et al., 1996). Neurotrophins like BDNF and NGF are critical for a wide variety of cellular processes including apoptotic suppression, differentiation, activity-dependent plasticity, and maintenance of synaptic connectivity (Bothwell, 2014). As a result, retrograde axonal transport of neurotrophins by BFCNs is crucial for their proper function and survival. NGF receptor alterations have been observed before phenotypic alteration of BFCNs in AD, suggesting that a lack of neurotrophic support is causative with respect to basal forebrain degeneration (Mufson et al., 2000, 2003). In postmortem AD BFCN, tropomyosin-related kinase A (TrkA) receptor is lost whereas the pan-neurotrophin receptor ($p75^{NTR}$) and tropomyosin-related kinase B (TrkB) receptors are stable (Counts et al., 2004; Ginsberg et al., 2006; Mufson et al., 2000). Increased NGF-like immunoreactivity has been found in both the AD cortex and hippocampus, with decreased levels in the basal forebrain, suggesting a deficit in retrograde axonal NGF transport (Scott et al., 1995). Impaired NGF transport in BFCNs has also been demonstrated in the amyloid

* Corresponding author at: Department of Psychiatry and Behavioural Neurosciences, McMaster University, 1280 Main Street West, Hamilton, Ontario L8S 4K1, Canada. Tel.: +1 905 525 9140 ×- 23344; fax: +1 905 522 8804.
E-mail address: fahnest@mcmaster.ca (M. Fahnestock).

0197-4580/$ – see front matter © 2019 Elsevier Inc. All rights reserved.
https://doi.org/10.1016/j.neurobiolaging.2019.07.018

precursor protein overexpressing Ts65Dn Down syndrome mouse model (Cooper et al., 2001; Salehi et al., 2006). These results implicate dysfunctional BFCN retrograde axonal transport in AD pathogenesis.

Aside from AD, age itself has been shown to negatively impact the basal forebrain. BFCN nuclear size and overall BFCN numbers are decreased in aged rats (Altavista et al., 1990). TrkA receptor levels, the receptor for NGF, and levels of downstream NGF signaling proteins are decreased in aged rat BFCNs (Parikh et al., 2013; Williams et al., 2006, 2007). The length of cholinergic fibers projecting to the hippocampus from the basal forebrain is reduced with age (Ypsilanti et al., 2008). Moreover, general retrograde axonal transport is diminished in aged rat BFCNs (Bearer et al., 2018; Cooper et al., 1994; De Lacalle et al., 1996). These deficits have behavioral consequences, as both aged rats and Lim Homebox-7 (LHX7) knockout mice that fail to develop forebrain cholinergic neurons show learning and memory impairments (Fragkouli et al., 2005; Gustilo et al., 1999).

Although aging has been demonstrated to impact general axonal transport in the basal forebrain, the impact of aging on neurotrophin-specific transport is poorly understood. Although both proBDNF and BDNF are found in the CNS (Michalski and Fahnestock, 2003), the form of NGF found in both human and rodent brain is proNGF (Fahnestock et al., 2001). ProNGF binds to TrkA and activates mitogen-activated protein kinase and Akt pathways to signal survival and neurite outgrowth (Clewes et al., 2008; Fahnestock and Shekari, 2019; Fahnestock et al., 2004; Ioannou and Fahnestock, 2017; Masoudi et al., 2009). ProNGF is retrogradely transported by peripheral dorsal root ganglion neurons (DRGs) and colocalizes with TrkA and $p75^{NTR}$ in DRG axons (De Nadai et al., 2016). However, proNGF axonal transport in the CNS has not been reported in the literature. BDNF retrograde transport has been demonstrated in both cortical and hippocampal neurons, but not in BFCNs (Poon et al., 2011; Zhao et al., 2014). As a result, we sought to explore the impact of age on proNGF and BDNF axonal transport in BFCNs.

To study transport in BFCNs, we adopted a microfluidic platform to separate neuronal cell bodies from axons. To model aging, cells were assayed after either 7–10 days in vitro (DIV), just enough time to allow axons to cross the 450 μM microgroove barrier, or 18–20 DIV. Aging in vitro is not a perfect analog of in vivo aging, but it is commonly used in both primary neuron and stem cell cultures to examine age-sensitive phenomena (Campos et al., 2014; Martin et al., 2008; Palomer et al., 2016; Sodero et al., 2011; Uday Bhanu et al., 2010). To confirm an aging phenotype in our neurons, BFCNs were stained with senescence-associated beta-galactosidase (SaβG), a well-validated marker of aging in humans, primates, and rodents both in vivo and in vitro (Dimri et al., 1995; Kurz et al., 2000; Mishima et al., 1999; Uday Bhanu et al., 2010).

2. Methods

All reagents were purchased from ThermoFisher Scientific (Burlington, Ontario, Canada) unless otherwise stated.

2.1. Neuron culture in microfluidic chambers

One day before dissection, microfluidic chambers (Xona Microfluidics, Temecula, CA, USA) were prepared according to the manufacturer's instruction. Briefly, 95% ethanol was added to each well of the chamber, followed by 2 phosphate-buffered saline (PBS) washes. One hundred microliters of poly-L-lysine (Sigma-Aldrich, Burlington, Ontario, Canada) was added to each of the wells, and the chambers were left to incubate overnight in an incubator at 37 °C and 5% CO_2. The chambers were then washed once with PBS, and 150 μL of cell culture medium was added to each of the wells. The cell culture medium consisted of Neurobasal, 1% Penicillin-Streptomycin, 1X B27 supplement, 1X GlutaMAX supplement, 1% fetal bovine serum, 50 ng/mL BDNF (Peprotech, Rocky Hill, NJ), and 50 ng/mL NGF (generous gift from Dr Michael Coughlin, McMaster University, Hamilton, Canada). The chambers were left to incubate at 37 °C and 5% CO_2 during the dissection.

Whole basal forebrain and cortex were dissected from embryonic day 18 rat embryos and immediately placed on ice in a solution of Hank's balanced salt solution with 1% Penicillin-Streptomycin. The tissue from 5 embryos was pooled for each round of dissection; therefore, sex was not determined. The neural tissue was washed with fresh Hank's balanced salt solution 5 times and then trypsinized in a water bath at 37 °C for 20 minutes. DNase I (Sigma-Aldrich) was added to a final concentration of 1×, and the tissue was triturated using a sterile, small-bore, fire-polished, glass pipette. Then 1 mL of cell culture medium was added, and the suspension was centrifuged at 250*g* for 4 minutes. The cell pellet was resuspended in 300 μL of cell culture medium, and the volume was adjusted to a final concentration of 1.0×10^6 cells/mL. After this, 140 μL of medium was removed from each of the 4 wells of the chambers, and 10 μL of cell suspension was added to the 2 left wells. The chambers were incubated for 10 minutes to allow cell adherence, which was confirmed under a microscope (Zeiss AxioVert A1). Then 150 μL of cell culture medium was added to all wells, and the cells were incubated overnight at 37 °C and 5% CO_2. The next day, all the medium was removed and replaced with a serum-free variant of the medium described previously. Cells were maintained in this medium for the duration of the experiments, with medium changes occurring every 48–72 hours.

2.2. Immunostaining and confirmation of BFCN phenotype

Neurons were stained for TrkA, TrkB, $p75^{NTR}$, and vesicular acetylcholine transporter (VAChT). Immunostaining was carried out in the microfluidic devices themselves. Cells were fixed in freshly prepared 4% paraformaldehyde for 30 minutes at room temperature (RT). Cells were washed 2 times with PBS, permeabilized with 0.2% Triton-X100 in PBS for 30 minutes at RT and blocked with 3% bovine serum albumin in PBS for 30 minutes at RT. Primary antibodies anti-TrkA (Santa Cruz Biotechnology, Santa Cruz, CA) or anti-VAChT (Santa Cruz Biotechnology) were added at a 1:500 dilution, anti-TrkB (Cell Signaling Technologies, Danvers, MA, USA) at a 1:500 dilution, and anti-$p75^{NTR}$ (Cell Signaling Technologies) at a 1:1600 dilution and were left to incubate overnight at 4 °C. Cells were washed with blocking solution 3 times on the following day. Alexa Fluor 488 secondary antibody was then added at a 1:1000 dilution and was left to incubate for 2 hours at RT. Neurons were visualized via fluorescence microscopy using a yellow fluorescent protein filter cube set (488 nm excitation, 525 nm emission). All immunostaining was carried out in microfluidic chambers between DIV10 and DIV18. TrkA and VAChT staining was robust at DIV10 (Supplementary Fig. 1A and B). Cortical neurons, as expected, did not express either and were used as a negative control (Supplementary Fig. 1C).

2.3. Histologic staining

Neurons were stained for SaβG at DIV7–10 and at DIV18–20. Cells were stained within the chambers themselves, with 150 μL of fixative added to all wells, followed by 150 μL of staining solution prepared according to the manufacturer's instruction (Cell Signaling). Cells were imaged using a Zeiss AxioVert A1 microscope.

2.4. Preparation of labeled neurotrophins

2.4.1. BDNF

Biotinylated BDNF was purchased from Alomone Labs (Tel Aviv, Israel). BDNF-biotin was incubated with Quantum Dot 625 Streptavidin conjugate at a 1:1 molar ratio on ice for 1 hour in the dark, and then diluted to 1 nM using serum-free cell culture medium without BDNF and NGF.

2.4.2. proNGF

We use a cleavage-resistant proNGF mutant containing a cytosine-to-guanine point mutation at position 633, resulting in an arginine-to-glycine substitution at the −1 position (ProNGF[R-1G]; Fahnestock et al., 2004). This cleavage-resistant proNGF binds to TrkA and $p75^{NTR}$, is internalized, and activates mitogen-activated protein kinase and Akt pathways (Fahnestock et al., 2004; Ioannou and Fahnestock, 2017; Masoudi et al., 2009). This sequence was engineered to include both a biotin-accepting Avi and a nickel-binding histidine tag, as described in Sung et al. (2011). Briefly, a vector containing proNGF-Avi (a generous gift from Dr Chengbiao Wu, UCSD) was digested using *Eco*R1 and *Bam*H1, and the excised proNGF-Avi fragment was ligated into a pcDNA 3.1 myc.his(+) vector. The R-1G mutation was then introduced using site-directed mutagenesis as described in Fahnestock et al. (2004) using the QuikChange II site-directed mutagenesis kit from Agilent Technologies (Santa Clara, CA, USA).

One microgram of the tagged proNGF[R-1G] plasmid, along with 20 μg of a plasmid encoding biotin ligase (a generous gift from Dr Chengbiao Wu, USCD), was cotransfected into HEK293FT cells using Lipofectamine 3000. Cells were grown to 70% confluency in medium containing Dulbecco's minimal essential medium, 1% fetal bovine serum, 1% Penicillin-Streptomycin, 200 mM GlutaMAX supplement, 50 μM D-biotin (Sigma-Aldrich), and 100 mM sodium pyruvate (Sigma-Aldrich). Medium was collected 72 hours post-transfection. ProNGF-biotin was purified from the medium via nickel affinity chromatography. Protein concentration was determined via an in-house NGF enzyme-liked immunosorbent assay (Fahnestock et al., 2004). Biotinylated proNGF was shown to be intact by Western blotting (Supplementary Fig. 2) and was labeled with Quantum Dot 625 as described previously for BDNF.

2.5. Tracking neurotrophin transport

2.5.1. BDNF

Neuronal cell bodies and axons were starved of neurotrophin by incubating overnight in medium containing only Neurobasal, 1% Penicillin-Streptomycin, 1X B27 supplement, and 1X GlutaMAX supplement. The next day, cells were washed 3 times with this neurotrophin-free medium to remove any residual neurotrophins. To the axonal side of the chambers was added 160 μL of 1 nM quantum dot-labeled BDNF (QD-BDNF) and was incubated for 1 hour (BFCNs) or 4 hours (cortical neurons) to account for differences in BDNF uptake efficiency between the cell types. The chambers were then transferred to an EVOS2 FL Microscope (ThermoFisher Scientific) with an environmental chamber set to 37 °C and 5% CO_2. QDs were visualized using a TexasRed filter, exciting at 585 nm and detecting emission at 624 nm. Kymographs were generated by compiling 120 images (from the TexasRed filter only) taken every 2 seconds into a vertical Z-stack using ImageJ. Particle speeds and pause duration were calculated using the mTrackJ ImageJ plug-in to track the distance traveled by labeled particles between images. Experiments were repeated 3 times.

2.5.2. proNGF

BFCN cell bodies were starved of neurotrophins as described previously, and 160 μL of 50 pM quantum dot-labeled proNGF (QD-proNGF) was added to the axons immediately and incubated for 1 hour. The same microscope described previously was used to capture the proNGF data. Mean fluorescence intensity was determined by measuring the mean gray value of pixels within proNGF-positive cell bodies with ImageJ. Experiments were repeated 3 times.

2.6. Statistical analysis

Sample sizes were similar to those reported in other related publications (Mufson et al., 2000; Poon et al., 2011; Zhao et al., 2014). Unpaired, 2-tailed Student's *t* tests were performed when comparing 2 groups, with a confidence interval of 95%. One-way analysis of variance (ANOVA) with post hoc Tukey tests was performed when more than 2 groups were compared, with a p value of 0.05 being considered significant. All error bars represent the standard error of the mean. Statistical methods are further elaborated on in the text and in all figure legends.

3. Results

3.1. BDNF transport is impaired in aged BFCNs but not cortical neurons

To determine the effect of aging in vitro on retrograde neurotrophin transport in BFCNs, axonal transport assays using QD-BDNF were carried out and kymographs were generated using neurons kept in culture for differing lengths of time. DIV8 BFCNs (Fig. 1A–C) and DIV22 cortical neurons (Fig. 1G–I) showed robust BDNF transport as indicated by sloped diagonal lines in the kymographs, whereas QD-BDNF taken up by DIV21 BFCNs were largely stationary as shown by the vertical lines (Fig. 1D–F). Quantification of QD-BDNF particle movement (Fig. 2A and B) demonstrated that the speed of QD-BDNF particles decreased significantly in DIV18–20 BFCNs compared with DIV7–10 BFCNs (N =60 QD-BDNF particles per group, $p = 0.003$, 1-way ANOVA and post hoc Tukey test). However, QD-BDNF particle speed did not differ between DIV7–10 BFCNs and DIV18 cortical neurons (N = 60 QD-BDNF particles per group $p = 0.9$, 1-way ANOVA and post hoc Tukey test). QD-BDNF particles also paused for significantly longer in DIV18–20 BFCNs compared with DIV7–10 BFCNs (N = 60 QD-BDNF particles per group, $p < 0.001$, 1-way ANOVA and post hoc Tukey test). QD-BDNF particles in DIV18–20 cortical neurons did not differ significantly in pause duration from DIV7–10 BFCNs (N = 60 QD-BDNF particles per group, $p = 0.928$, 1-way ANOVA and post hoc Tukey test). BDNF transport did not decrease significantly with further in vitro aging, as DIV21–24 BFCNs were not significantly different from DIV18–20 BFCNs in terms of BDNF speed and pause duration (data not shown).

3.2. proNGF uptake is robust in young BFCNs and is reduced with age in vitro

Next, we aimed to characterize proNGF transport in BFCNs and to assess the role of in vitro aging on the process. To determine if similar axonal transport deficits could be seen with proNGF, experiments were repeated using the same time points with cleavage-resistant proNGF as opposed to BDNF. Of note, cortical neurons could not be used as a comparison group because of their lack of TrkA expression.

The conditions required for proNGF uptake differed from BDNF: neurotrophic starvation of axon terminals and cell bodies, as carried out for BDNF, resulted in no proNGF being taken up by BFCNs; proNGF transport occurred only after cell bodies alone instead of axon terminals and cell bodies were starved of neurotrophins

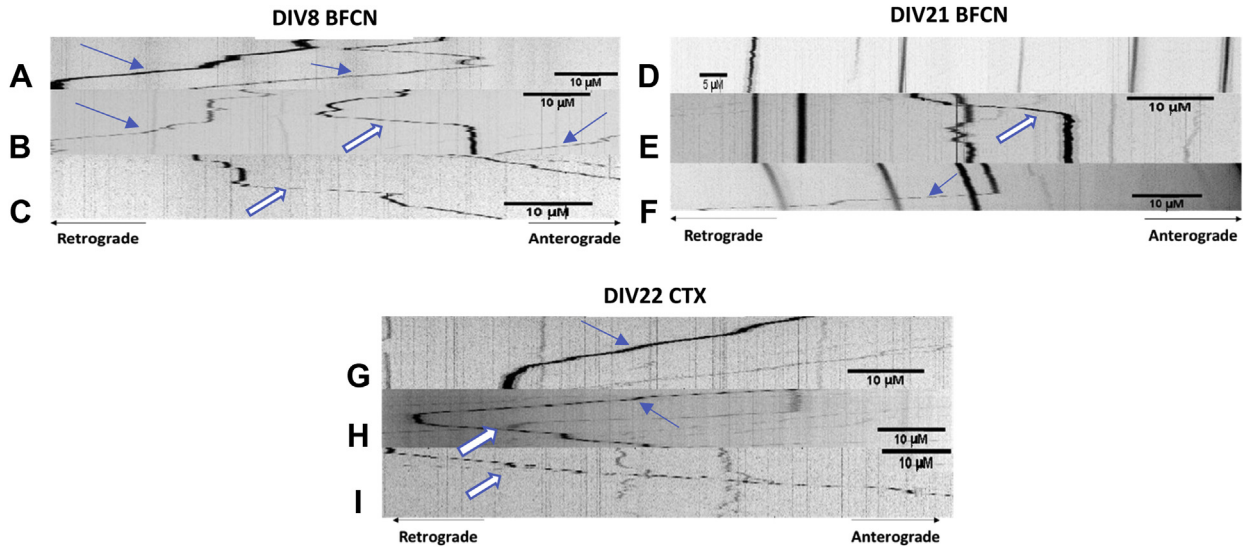

Fig. 1. BDNF transport in BFCNs and CTXs aged in culture. Kymographs of quantum dot–labeled BDNF (QD-BDNF) particles within the microgrooves of BFCNs (A–F) and CTXs (G–I) in microfluidic chambers. Sloped lines represent movement in the anterograde or retrograde direction as indicated by open or closed arrows, respectively. Vertical line segments indicate instances of no movement or pausing. Neurons were cultured for at least 7 DIV to allow axons to fully traverse the microgrooves. Images were taken 1 hour after 1 nM QD-BDNF was added to the axon terminal side only. Aged (DIV21) BFCNs clearly show stationary QD-BDNF (D–F). Abbreviations: BDNF, brain-derived neurotrophic factor; BFCN, basal forebrain cholinergic neuron; CTX, cortical neuron; DIV, days in vitro.

(Fig. 3A and B). We also determined that proNGF uptake by DIV7–10 BFCNs was extremely rapid. ProNGF uptake occurred within 15 minutes of its administration, and it accumulated in cell bodies after just 1 hour (Figs. 3A and 4A). ProNGF uptake in DIV7–10 BFCNs was also extremely robust, as just 50 pM proNGF was enough to yield a QD-proNGF signal along the entire length of the BFCN axons (Figs. 3A and 4C). For comparison, BDNF uptake was undetectable at 50 pM (data not shown), and transport required at least 1 nM BDNF and starvation of both axons and cell bodies (Fig. 3C and D).

Next, we assessed the effect of in vitro aging on proNGF uptake. Experiments were completed at DIV7–10 and DIV18–20, with the only difference being the starvation conditions required for proNGF uptake as described previously; cell bodies were starved of neurotrophins and QD-proNGF was added immediately to the axonal compartment. ProNGF accumulation in DIV18–20 BFCN cell bodies was significantly diminished compared with DIV7–10 BFCNs (Figs. 4A, B and 5, N = 100 cell bodies, $p < 0.001$, Student's t test).

3.3. Aged BFCNs stain positive for SaβG

To determine if neurons cultured for extended periods of time displayed signs of aging, we carried out histologic staining for SaβG. BFCNs cultured for 10 DIV did not stain for SaβG (Fig. 6A). Only BFCNs cultured for 18 days or more stained positive for SaβG (Fig. 6B and C). Staining became more pronounced as the neurons were kept longer in culture, with DIV21–24 BFCNs demonstrating robust SaβG staining (Fig. 6C). Cortical neurons did not stain positive for SaβG even at DIV24 (Fig. 6D and E).

3.4. TrkB immunoreactivity is decreased in BFCNs but not cortical neurons aged in vitro

To determine if a reduction in the BDNF receptor TrkB was facilitating the impaired BDNF transport in aged BFCNs, immunostaining for TrkB was carried out at both time points. DIV18 BFCNs displayed significantly reduced TrkB immunoreactivity compared

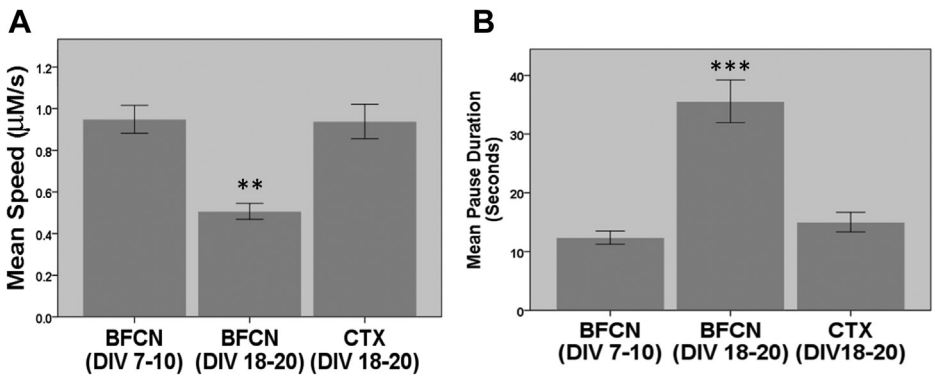

Fig. 2. BDNF transport speed and pause duration in basal forebrain BFCNs and CTXs aged in culture. Quantification of speed (A) and pause duration (B) of quantum dot-labeled BDNF (QD-BDNF) in basal forebrain cholinergic neurons (BFCNs) and CTXs. Data were collected 1 hour after 1 nM QD-BDNF was added to the axon terminal side of the microfluidic chambers for BFCNs, and 4 hours for CTXs. Neurons cultured for either 7–10 days in vitro (DIV) or 18–20 DIV. The mTrackJ plug-in for ImageJ was used to determine the distanced traveled by QD-BDNF particles between time-lapse images. Each bar shows N = 60 QD-BDNF particles from 3 different chambers and 3 rounds of dissection (5 embryos each). Data are represented as the mean ± SE. $^{**}p < 0.01$, $^{***}p < 0.001$, 1-way ANOVA and post hoc Tukey test. Abbreviations: ANOVA, analysis of variance; BDNF, brain-derived neurotrophic factor; BFCN, basal forebrain cholinergic neuron; CTX, cortical neuron; DIV, days in vitro; SE, standard error.

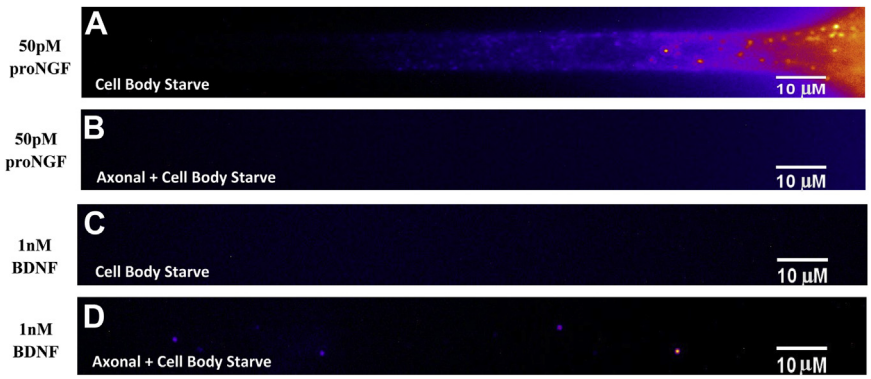

Fig. 3. Representative uptake of neurotrophins in BFCNs. proNGF uptake (C) by BFCNs is more robust than BDNF uptake (A and B). proNGF uptake conditions differ from BDNF (A–D). All images were taken at the first instance of fluorescence in the microgrooves after quantum dot (QD)-labeled neurotrophin administration to axon terminals only. For QD-BDNF, images were taken 1 hour after neurotrophin addition following starvation of axons and cell bodies overnight. For QD-proNGF, images were taken 15 minutes after starvation of cell bodies only followed by immediate QD-proNGF addition. Individual microgrooves visualized. Abbreviation: BDNF, brain-derived neurotrophic factor; BFCN, basal forebrain cholinergic neuron; NGF, nerve growth factor.

with DIV10 (Fig. 7A, B, and E, N = 60 cell bodies, $p < 0.001$, 1-way ANOVA and post hoc Tukey test). TrkB immunoreactivity in cortical neurons did not change significantly with in vitro age (Fig. 7C–E, N = 60 cell bodies, $p = 0.8$, 1-way ANOVA and post hoc Tukey test). TrkB immunoreactivity in DIV10 BFCNs was significantly higher compared with cortical neurons at both DIV10 and DIV18 (Fig. 7A, C–E) N = 60 cell bodies, $p < 0.001$, 1-way ANOVA and post hoc Tukey test).

3.5. TrkA, but not $p75^{NTR}$, immunoreactivity is decreased in BFCNs aged in vitro

To determine if a reduction in proNGF receptors TrkA and $p75^{NTR}$ was mediating the reduced proNGF uptake in DIV18–20 BFCNs, immunostaining for TrkA and $p75^{NTR}$ was carried out at both time points. TrkA immunoreactivity was significantly reduced in BFCNs at DIV18 compared with DIV10 (Fig. 8, N = 60 cell bodies, $p < 0.001$, Student's t test), whereas $p75^{NTR}$ immunoreactivity did not change significantly between the 2 time points (Fig. 9, $N = 60$ cell bodies, $p = 0.09$, Student's t test).

4. Discussion

Here, we characterized neurotrophin axonal transport and neurotrophin receptor expression in BFCNs. We demonstrated that both BDNF transport and proNGF transport diminish with in vitro aging in BFCNs and that BDNF transport deficits are unique to BFCNs. For BDNF, significant increases in pause duration and decreases in axonal transport speed were seen in DIV18–20 BFCNs but not in younger BFCNs or in DIV18–20 cortical neurons. Cortical neurons whose axons were clearly degenerated (e.g., whose axons were no longer smooth and continuous) ceased to take up BDNF only at DIV28. For proNGF, levels of uptake were significantly diminished in DIV20 BFCNs compared with DIV8 BFCNs. BFCNs cultured for 18 days or more, but not cortical neurons, stained positive for SaβG and were the only neurons that displayed

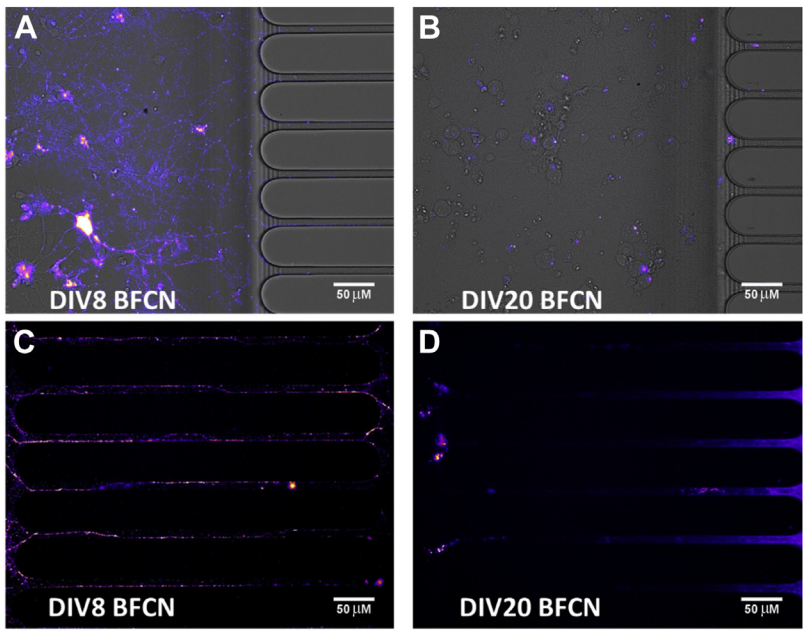

Fig. 4. Uptake and transport of quantum dot-labeled proNGF (QD-proNGF) in BFCNs. Data were collected 1 hour after 50 pM QD-proNGF[R-1G] was added to the axon terminal side of the microfluidic chambers. (A and B) Cell bodies; (C and D) microgrooves (axons). Abbreviations: DIV, days in vitro; NGF, nerve growth factor.

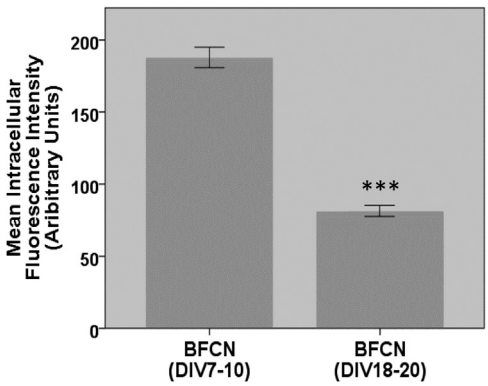

Fig. 5. Quantification of quantum dot-labeled proNGF (QD-proNGF) uptake by BFCNs. BFCN cell bodies demonstrated more proNGF[R-1G] at DIV8 compared with DIV20. N = 100 cell bodies per group, from 3 different chambers and 2 rounds of dissection (5 embryos each). Data are represented as the mean ± SE. ***$p < 0.001$ by Student's t test. Abbreviations: DIV, days in vitro; NGF, nerve growth factor; SE, standard error.

neurotrophic transport deficits. BFCNs aged in vitro displayed significantly reduced TrkA and TrkB immunoreactivity. $p75^{NTR}$ immunoreactivity did not change significantly in BFCNs aged in vitro. These findings strongly suggest that BFCNs are particularly susceptible to senescence and age-induced neurotrophin transport deficits and to TrkA and TrkB receptor downregulation.

BFCNs were much more efficient in their uptake of BDNF compared with their cortical counterparts. We found that cortical neurons required a 4-hour incubation with QD-BDNF in order for transport within the microgrooves to be observed, in line with previously reported findings in hippocampal neurons (Poon et al., 2011; Zhao et al., 2014). BFCNs, on the other hand, required only 1 hour of incubation time. This is most likely because of the greater TrkB expression observed in BFCNs compared with cortical neurons. BDNF uptake was slower in DIV18 BFCNs (data not shown) compared with DIV10, further implicating TrkB levels in BDNF uptake latency. Once taken up, transport speed (1 μM/s) and mean pause duration (12.4 seconds) of BDNF by DIV10 BFCNs were similar to both cortical and hippocampal neurons (Poon et al., 2011; Zhao et al., 2014). Reduced TrkB receptor levels do not account for the decreased motility of BDNF particles in DIV18 BFCNs because DIV18 cortical neurons displayed significantly less TrkB immunoreactivity compared with DIV10 BFCNs, but their BDNF transport dynamics did not differ. Although differences in TrkB expression may explain the variance in BDNF uptake efficiency between cell types, the mechanism of decreased BDNF motility along axons with increased in vitro age remains unknown.

The efficiency of BFCN neurotrophin transport was even more evident with proNGF than with BDNF, with proNGF uptake beginning within 10 minutes of neurotrophin addition to BFCN axon terminals. This time course was even faster than in DRGs, a class of neurons in which proNGF transport is well characterized. In DRGs, proNGF transport occurs after 35 minutes (De Nadai et al., 2016; Villarin et al., 2016). Taken together, these results suggest that both CNS and peripheral nervous system neurons are capable of rapid proNGF uptake and subsequent retrograde axonal transport. The functional implications of this rapid uptake are currently unknown.

The conditions required for uptake differed between BDNF and proNGF. For BDNF, both axons and cell bodies were deprived of neurotrophin for at least 1 hour before uptake was observed. For proNGF, depriving both the axons and cell bodies of neurotrophin completely inhibited uptake. This finding suggests that TrkA trafficking in BFCNs is similar to DRGs, where NGF-bound TrkA promotes the recruitment of additional TrkA receptors to axon terminals in a positive feedback loop (Yamashita et al., 2017). Cutting off neurotrophin supply to the axons abolishes this positive feedback loop, reducing TrkA trafficking to the terminals. This finding also suggests that TrkA and TrkB trafficking are governed by distinct mechanisms in BFCNs, because axonal neurotrophin starvation abolishes TrkA-mediated (proNGF) transport but not TrkB-mediated (BDNF) transport (Zhao et al., 2014).

The uptake of proNGF was diminished in BFCNs aged in vitro. This diminished uptake coincided with a significant decrease in TrkA receptor immunoreactivity. $p75^{NTR}$ immunoreactivity did not decrease with in vitro age. These findings suggest that the reduction in TrkA receptor levels is responsible for the reduced uptake of proNGF by BFCNs aged in vitro. $p75^{NTR}$ has a higher binding affinity for proNGF compared with TrkA (Clewes et al., 2008; Nykjaer et al.,

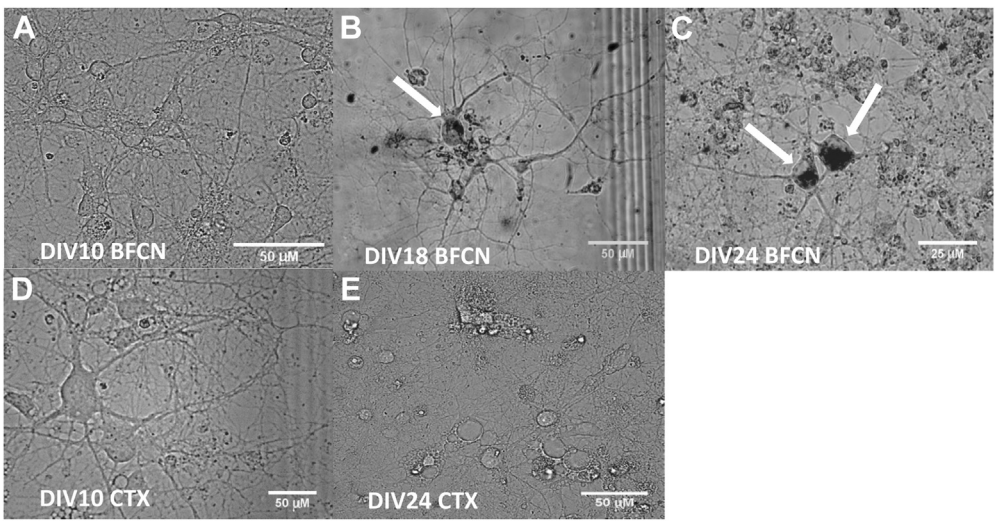

Fig. 6. Senescence-associated beta-galactosidase stain of BFCN and (CTX) aged in culture. DIV10 BFCNs and CTXs do not stain for senescence-associated beta-galactosidase (A and D). BFCNs begin to stain positive at DIV18, with more pronounced staining occurring at DIV24 (B and C). DIV24 CTXs do not stain positive for senescence-associated beta-galactosidase (E). Arrows indicate labeled cell bodies. Abbreviations: BFCN, basal forebrain cholinergic neuron; CTX, cortical neuron; DIV, days in vitro.

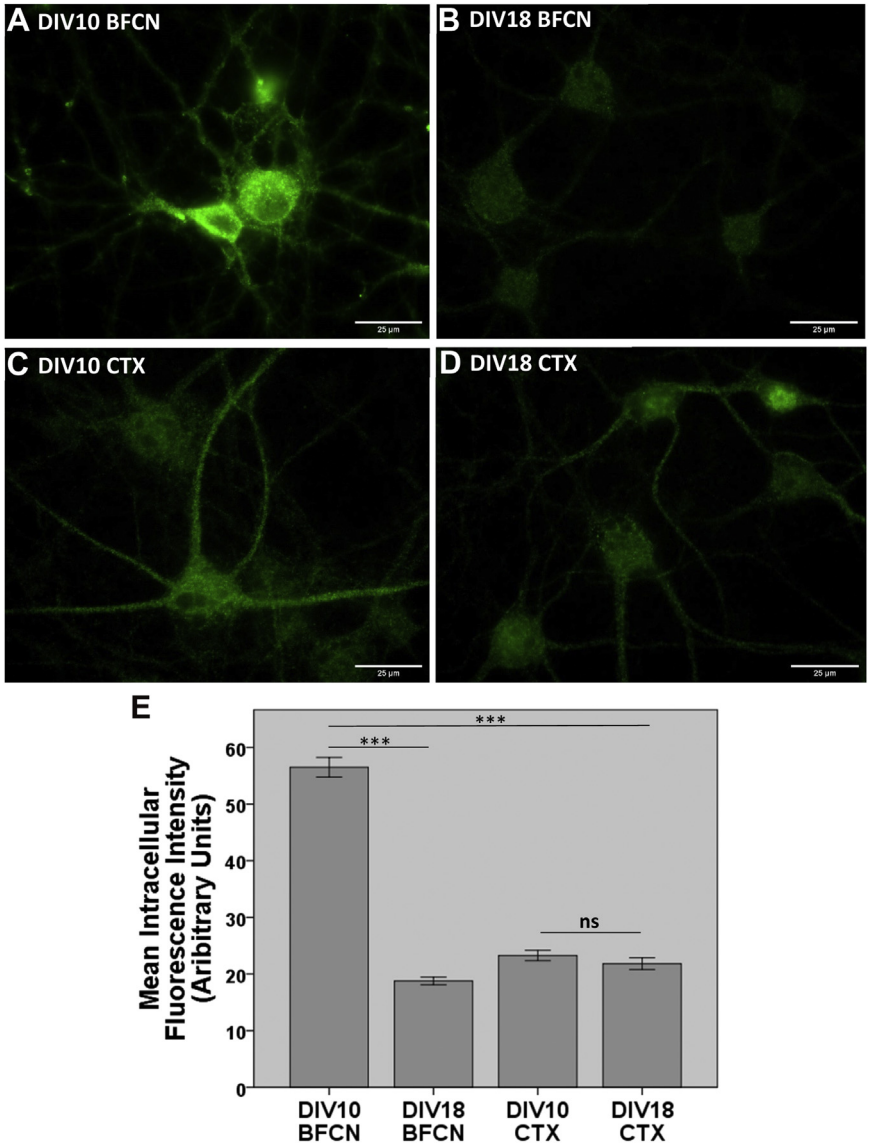

Fig. 7. Decreased TrkB immunoreactivity in BFCNs but not CTXs aged in vitro. BFCN cell bodies demonstrated significantly less TrkB immunoreactivity at DIV18 (B) compared with DIV10 (A). TrkB immunoreactivity did not change significantly in CTXs between DIV10 (C) and DIV18 (D). TrkB immunoreactivity was significantly greater in BFCNs at DIV10 (A) compared with CTXs at all time points (C,D). Quantification in (E). Each bar shows N = 60 cell bodies from 3 different chambers and 3 rounds of dissection (5 embryos each). Data are represented as the mean ± SE. $^{***}p < 0.001$, "ns" = not significant ($p = 0.8$) 1-way ANOVA and post hoc Tukey test. Abbreviations: ANOVA, analysis of variance; BFCN, basal forebrain cholinergic neuron; CTX, cortical neuron; DIV, days in vitro; SE, standard error; TrkB tropomyosin-related kinase B.

2004). However, its maintenance in DIV18 BFCNs did not result in maintenance of proNGF transport at this time point, suggesting that the balance between TrkA and $p75^{NTR}$ levels is important for the retrograde transport of proNGF and that loss of TrkA contributes to reduced proNGF transport in aged BFCNs.

Although the uptake of proNGF was diminished in aged BFCNs, the robust level of uptake observed in young BFCNs was surprising. To observe a QD-proNGF signal along the entire length of the microgrooves 50 pM of proNGF was enough. This rapid and robust uptake of proNGF made generating kymographs with individual trackable particles difficult. With BDNF, even concentrations of over 1 nM resulted in few particles populating the microgrooves. These results strongly suggest that proNGF uptake is more efficient than BDNF uptake in BFCNs.

One of the key limitations of this work is the in vitro model of aging. Cultured CNS neurons are viable for 3–4 weeks in culture before they degenerate. With the lifespan of healthy rats being around 2 years, the degeneration seen in vitro occurs at an accelerated rate compared with in vivo. However, many of the hallmarks associated with neuronal aging in vivo are recapitulated in vitro. Hippocampal neurons kept in culture for 3 weeks display reactive oxygen species accumulation, lipofuscin granules, loss of cholesterol from cell membranes, and activation of both the phosphorylated c-Jun N-terminal kinase and p53/p21 pathways, all of which are also seen in neurons taken from aged animals (Brewer et al., 2007; Calvo et al., 2015; Porter et al., 1997; Sodero et al., 2011). Furthermore, it has recently been demonstrated that general axonal transport through the septohippocampal tract is reduced in vivo with normal aging in mice and is exacerbated by AD pathology (Bearer et al., 2018). Our BFCNs, but not cortical neurons, stained positive for SaβG at DIV18, a well-validated marker of aging both in vivo and in vitro. By DIV28, axons were clearly degenerating in both groups. TrkA downregulation in the absence of $p75^{NTR}$ downregulation has been repeatedly observed in both aging and

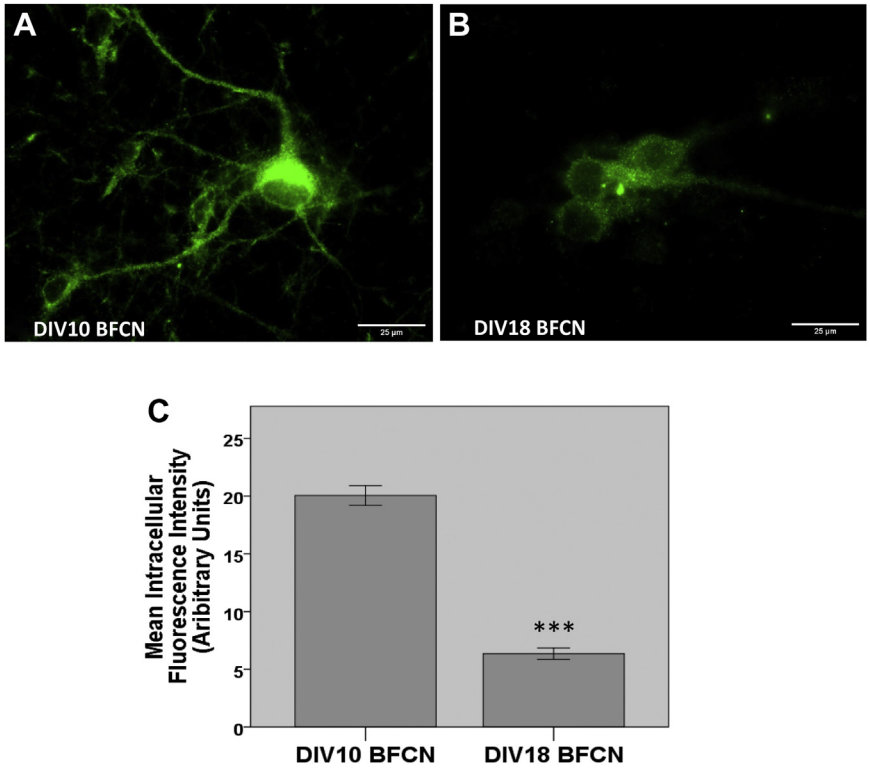

Fig. 8. Decreased TrkA immunoreactivity in BFCNs aged in vitro. BFCN cell bodies demonstrated significantly less TrkA immunoreactivity at DIV18 (B) compared with DIV10 (A). Quantification in (C). N = 60 cell bodies per group, from 3 different chambers and 3 rounds of dissection (5 embryos each). Data are represented as the mean ± SE. ***$p < 0.001$ by Student's *t* test. Abbreviations: BFCN, basal forebrain cholinergic neuron; DIV, days in vitro; SE, standard error; TrkA, tropomyosin-related kinase A.

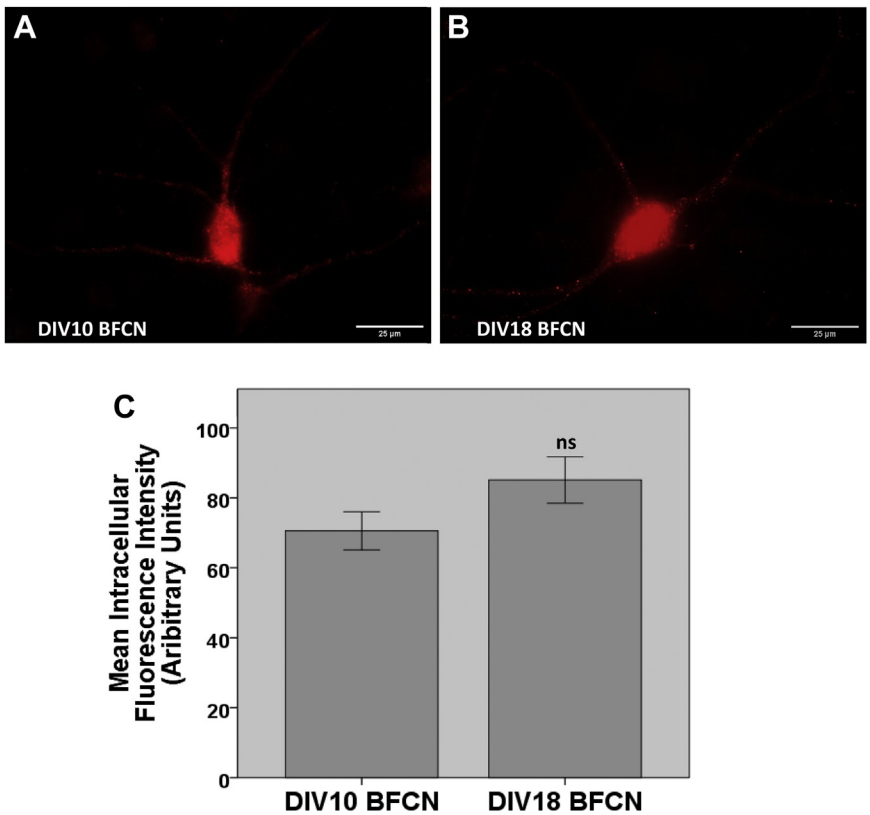

Fig. 9. $p75^{NTR}$ immunoreactivity in BFCNs does not change during aging in vitro. $p75^{NTR}$ immunoreactivity did not change significantly between DIV10 (A) and DIV18 (B) in BFCNs. Quantification in (C). N = 60 cell bodies per group, from 3 different chambers and 3 rounds of dissection (5 embryos each). Data are represented as the mean ± SE. $p = 0.09$ by Student's *t* test. ns = not significant ($p = 0.8$). Abbreviations: BFCN, basal forebrain cholinergic neuron; DIV, days in vitro; $p75^{NTR}$, pan-neurotrophin receptor; SE, standard error.

AD-affected basal forebrain neurons in humans and rodents (Fahnestock and Shekari, 2019; Gibbs, 1998; Ginsberg et al., 2006; Mufson et al., 2000; Niewiadomska et al., 2002). Thus, although the molecular mechanisms underlying neuronal degeneration in vivo are accelerated in vitro, they are not dissimilar. Studying in vitro aging provides an effective way to gain insight into the mechanisms underlying aging in paradigms where in vivo work is difficult.

In conclusion, our data suggest that BFCNs display unique, age-dependent deficits in TrkA and TrkB receptor expression and the retrograde axonal transport of BDNF and proNGF. These deficits support previous findings that demonstrate the susceptibility of the basal forebrain to age-related degeneration and may explain the extreme susceptibility of the basal forebrain to AD. The basal forebrain projects to almost all areas of the cortex and the hippocampus. It plays canonical and crucial roles in learning, memory, and attention and is also involved in other important functions including regulation of blood flow to the cortex. Understanding how and why these neurons degenerate both with age and in AD is critical for our understanding of aging, neurodegenerative diseases, and the nervous system as a whole.

Disclosure

The authors have no actual or potential conflicts of interest.

Acknowledgements

The authors are grateful to Drs Wayne Poon and Carl Cotman (UC Irvine) and Dr Chengbiao Wu (UCSD) for help with microfluidic chambers and transport assays.

This work was supported by grants to M.F. from the Alzheimer Society of Canada and the Canadian Institutes of Health Research (MOP-102723, PJT-159493), and by an Ontario Graduate Scholarship to A.S.

The data contained in this manuscript being submitted have not been previously published, have not been submitted elsewhere and will not be submitted elsewhere while under consideration at Neurobiology of Aging.

All authors have reviewed the contents of the manuscript, approved its contents, and validated the accuracy of the data.

Appendix A. Supplementary data

Supplementary data to this article can be found online at https://doi.org/10.1016/j.neurobiolaging.2019.07.018.

References

Altavista, M.C., Rossi, P., Bentivoglio, A.R., Crociani, P., Albanese, A., 1990. Aging is associated with a diffuse impairment of forebrain cholinergic neurons. Brain Res. 508, 51–59.

Baker-Nigh, A., Vahedi, S., Davis, E.G., Weintraub, S., Bigio, E.H., Klein, W.L., Geula, C., 2015. Neuronal amyloid-β accumulation within cholinergic basal forebrain in ageing and Alzheimer's disease. Brain 138, 1722–1737.

Ballinger, E.C., Ananth, M., Talmage, D.A., Role, L.W., 2016. Basal forebrain cholinergic circuits and signaling in cognition and cognitive decline. Neuron 91, 1199–1218.

Baxter, M.G., Chiba, A.A., 1999. Cognitive functions of the basal forebrain. Curr. Opin. Neurobiol. 9, 178–183.

Bearer, E.L., Manifold-Wheeler, B.C., Medina, C.S., Gonzales, A.G., Chaves, F.L., Jacobs, R.E., 2018. Alterations of functional circuitry in aging brain and the impact of mutated APP expression. Neurobiol. Aging 70, 276–290.

Bothwell, M., 2014. NGF, BDNF, NT3, and NT4. Handb. Exp. Pharmacol. 220, 3–15.

Brewer, L.D., Thibault, O., Staton, J., Thibault, V., Rogers, J.T., Garcia-Ramos, G., Kraner, S., Landfield, P.W., Porter, N.M., 2007. Increased vulnerability of hippocampal neurons with age in culture: temporal association with increases in NMDA receptor current, NR2A subunit expression and recruitment of L-type calcium channels. Brain Res. 1151, 20–31.

Calvo, M., Sanz-Blasco, S., Caballero, E., Villalobos, C., Núñez, L., 2015. Susceptibility to excitotoxicity in aged hippocampal cultures and neuroprotection by non-steroidal anti-inflammatory drugs: role of mitochondrial calcium. J. Neurochem. 132, 403–417.

Campos, P.B., Paulsen, B.S., Rehen, S.K., 2014. Accelerating neuronal aging in in vitro model brain disorders: a focus on reactive oxygen species. Front. Aging Neurosci. 6, 292.

Clewes, O., Fahey, M.S., Tyler, S.J., Watson, J.J., Seok, H., Catania, C., Cho, K., Dawbarn, D., Allen, S.J., 2008. Human ProNGF: biological effects and binding profiles at TrkA, P75NTR and sortilin. J. Neurochem. 107, 1124–1135.

Cooper, J.D., Lindholm, D., Sofroniew, M.V., 1994. Reduced transport of [125I]nerve growth factor by cholinergic neurons and down-regulated trka expression in the medial septum of aged rats. Neuroscience 62, 625–629.

Cooper, J.D., Salehi, A., Delcroix, J.-D., Howe, C.L., Belichenko, P.V., Chua-Couzens, J., Kilbridge, J.F., Carlson, E.J., Epstein, C.J., Mobley, W.C., 2001. Failed retrograde transport of NGF in a mouse model of Down's syndrome: reversal of cholinergic neurodegenerative phenotypes following NGF infusion. Proc. Natl. Acad. Sci. U. S. A. 98, 10439–10444.

Counts, S.E., Nadeem, M., Wuu, J., Ginsberg, S.D., Saragovi, H.U., Mufson, E.J., 2004. Reduction of cortical TrkA but not p75 NTR protein in early-stage Alzheimer's disease. Ann. Neurol. 56, 520–531.

De Lacalle, S., Cooper, J.D., Svendsen, C.N., Dunnett, S.B., Sofroniew, M.V., 1996. Reduced retrograde labelling with fluorescent tracer accompanies neuronal atrophy of basal forebrain cholinergic neurons in aged rats. Neuroscience 75, 19–27.

De Nadai, T., Marchetti, L., Di Rienzo, C., Calvello, M., Signore, G., Di Matteo, P., Gobbo, F., Turturro, S., Meucci, S., Viegi, A., Beltram, F., Luin, S., Cattaneo, A., 2016. Precursor and mature NGF live tracking: one versus many at a time in the axons. Sci. Rep. 6, 20272.

Dimri, G.P., Lee, X., Basile, G., Acosta, M., Scott, G., Roskelley, C., Medrano, E.E., Linskens, M., Rubelj, I., Pereira-Smith, O., 1995. A biomarker that identifies senescent human cells in culture and in aging skin in vivo. Proc. Natl. Acad. Sci. U. S. A. 92, 9363–9367.

DiStefano, P.S., Friedman, B., Radziejewski, C., Alexander, C., Boland, P., Schick, C.M., Lindsay, R.M., Wiegand, S.J., 1992. The neurotrophins BDNF, NT-3, and NGF display distinct patterns of retrograde axonal transport in peripheral and central neurons. Neuron 8, 983–993.

Fahnestock, M., Shekari, A., 2019. ProNGF and neurodegeneration in Alzheimer's disease. Front. Neurosci. 13, 129.

Fahnestock, M., Michalski, B., Xu, B., Coughlin, M.D., 2001. The precursor pro-nerve growth factor is the predominant form of nerve growth factor in brain and is increased in Alzheimer's disease. Mol. Cell. Neurosci. 18, 210–220.

Fahnestock, M., Yu, G., Michalski, B., Mathew, S., Colquhoun, A., Ross, G.M., Coughlin, M.D., 2004. The nerve growth factor precursor proNGF exhibits neurotrophic activity but is less active than mature nerve growth factor. J. Neurochem. 89, 581–592.

Ferreira-Vieira, H., Guimaraes, T.M., Silva, I.R., Ribeiro, F.M., 2016. Alzheimer's disease: targeting the cholinergic system. Curr. Neuropharmacol. 14, 101–115.

Fragkouli, A., Hearn, C., Errington, M., Cooke, S., Grigoriou, M., Bliss, T., Stylianopoulou, F., Pachnis, V., 2005. Loss of forebrain cholinergic neurons and impairment in spatial learning and memory in LHX7-deficient mice. Eur. J. Neurosci. 21, 2923–2938.

Gibbs, R.B., 1998. Impairment of basal forebrain cholinergic neurons associated with aging and long-term loss of ovarian function. Exp. Neurol. 151, 289–302.

Ginsberg, S.D., Che, S., Wuu, J., Counts, S.E., Mufson, E.J., 2006. Down regulation of trk but not p75NTR gene expression in single cholinergic basal forebrain neurons mark the progression of Alzheimer's disease. J. Neurochem. 97, 475–487.

Götz, J., Chen, F., van Dorpe, J., Nitsch, R.M., 2001. Formation of neurofibrillary tangles in P301l tau transgenic mice induced by Abeta 42 fibrils. Science 293, 1491–1495.

Grothe, M., Heinsen, H., Teipel, S.J., 2012. Atrophy of the cholinergic basal forebrain over the adult age range and in early stages of Alzheimer's disease. Biol. Psychiatry 71, 805–813.

Gustilo, M.C., Markowska, A.L., Breckler, S.J., Fleischman, C.A., Price, D.L., Koliatsos, V.E., 1999. Evidence that nerve growth factor influences recent memory through structural changes in septohippocampal cholinergic neurons. J. Comp. Neurol. 405, 491–507.

Ioannou, M.S., Fahnestock, M., 2017. ProNGF, but not NGF, switches from neurotrophic to apoptotic activity in response to reductions in TrKA receptor levels. Int. J. Mol. Sci. 18, E599.

Kurz, D.J., Decary, S., Hong, Y., Erusalimsky, J.D., 2000. Senescence-associated (beta)-galactosidase reflects an increase in lysosomal mass during replicative ageing of human endothelial cells. J. Cell Sci. 113, 3613–3622.

Linville, D.G., Arnerić, S.P., 1991. Cortical cerebral blood flow governed by the basal forebrain: age-related impairments. Neurobiol. Aging 12, 503–510.

Martin, M.G., Perga, S., Trovo, L., Rasola, A., Holm, P., Rantamaki, T., Harkany, T., Castren, E., Chiara, F., Dotti, C.G., 2008. Cholesterol loss enhances TrkB signaling in hippocampal neurons aging in vitro. Mol. Biol. Cell. 19, 2101–2112.

Masoudi, R., Ioannou, M.S., Coughlin, M.D., Pagadala, P., Neet, K.E., Clewes, O., Allen, S.J., Dawbarn, D., Fahnestock, M., 2009. Biological activity of nerve growth factor precursor is dependent upon relative levels of its receptors. J. Biol. Chem. 284, 18424–18433.

Michalski, B., Fahnestock, M., 2003. Pro-brain-derived neurotrophic factor is decreased in parietal cortex in Alzheimer's disease. Brain Res Mol Brain Res 111, 148–154.

Mishima, K., Handa, J.T., Aotaki-Keen, A., Lutty, G.A., Morse, L.S., Hjelmeland, L.M., 1999. Senescence-associated β-galactosidase histochemistry for the primate eye. Invest. Ophthalmol. Vis. Sci. 40, 1590–1593.

Mufson, E.J., Ma, S.Y., Cochran, E.J., Bennett, D.A., Beckett, L.A., Jaffar, S., Saragovi, H.U., Kordower, J.H., 2000. Loss of nucleus basalis neurons containing trkA immunoreactivity in individuals with mild cognitive impairment and early Alzheimer's diseases. J. Comp. Neurol. 427, 19–30.

Mufson, E.J., Ginsberg, S.D., Ikonomovic, M.D., DeKosky, S.T., 2003. Human cholinergic basal forebrain: chemoanatomy and neurologic dysfunction. J. Chem. Neuroanat. 26, 233–242.

Niewiadomska, G., Komorowski, S., Baksalerska-Pazera, M., 2002. Amelioration of cholinergic neurons dysfunction in aged rats depends on the continuous supply of NGF. Neurobiol. Aging 23, 601–613.

Nykjaer, A., Lee, R., Teng, K.K., Jansen, P., Madsen, P., Nielsen, M.S., Jacobsen, C., Kliemannel, M., Schwarz, E., Willnow, T.E., Hempstead, B.L., Petersen, C.M., 2004. Sortilin is essential for proNGF-induced neuronal cell death. Nature 427, 843–848.

Palomer, E., Martín-Segura, A., Baliyan, S., Ahmed, T., Balschun, D., Venero, C., Martin, M.G., Dotti, C.G., 2016. Aging triggers a repressive chromatin state at BDNF promoters in hippocampal neurons. Cell Rep. 16, 2889–2900.

Parikh, V., Howe, W.M., Welchko, R.M., Naughton, S.X., D'Amore, D.E., Han, D.H., Deo, M., Turner, D.L., Sarter, M., 2013. Diminished trkA receptor signaling reveals cholinergic-attentional vulnerability of aging. Eur. J. Neurosci. 37, 278–293.

Poon, W.W., Blurton-Jones, M., Tu, C.H., Feinberg, L.M., Chabrier, M.A., Harris, J.W., Jeon, N.L., Cotman, C.W., 2011. β-Amyloid impairs axonal BDNF retrograde trafficking. Neurobiol. Aging 32, 821–833.

Porter, N.M., Thibault, O., Thibault, V., Chen, K.C., Landfield, P.W., 1997. Calcium channel density and hippocampal cell death with age in long-term culture. J. Neurosci. 17, 5629–5639.

Salehi, A., Delcroix, J.D., Belichenko, P.V., Zhan, K., Wu, C., Valletta, J.S., Takimoto-Kimura, R., Kleschevnikov, A.M., Sambamurti, K., Chung, P.P., Xia, W., Villar, A., Campbell, W.A., Kulnane, L.S., Nixon, R.A., Lamb, B.T., Epstein, C.J., Stokin, G.B., Goldstein, L.S.B., Mobley, W.C., 2006. Increased app expression in a mouse model of down's syndrome disrupts NGF transport and causes cholinergic neuron degeneration. Neuron 51, 29–42.

Schmitz, T.W., Nathan Spreng, R., Weiner, M.W., Aisen, P., Petersen, R., Jack, C.R., Jagust, W., Trojanowki, J.Q., Toga, A.W., Beckett, L., Green, R.C., Saykin, A.J., Morris, J., Shaw, L.M., Khachaturian, Z., Sorensen, G., Kuller, L., Raichle, M., Paul, S., Davies, P., Fillit, H., Hefti, F., Holtzman, D., Mesulam, M.M., Potter, W., Snyder, P., Schwartz, A., Montine, T., Thomas, R.G., Donohue, M., Walter, S., Gessert, D., Sather, T., Jiminez, G., Harvey, D., Bernstein, M., Fox, N., Thompson, P., Schuff, N., Borowski, B., Gunter, J., Senjem, M., Vemuri, P., Jones, D., Kantarci, K., Ward, C., Koeppe, R.A., Foster, N., Reiman, E.M., Chen, K., Mathis, C., Landau, S., Cairns, N.J., Householder, E., Taylor-Reinwald, L., Lee, V., Korecka, M., Figurski, M., Crawford, K., Neu, S., Foroud, T.M., Potkin, S., Shen, L., Faber, K., Kim, S., Nho, K., Thal, L., Buckholtz, N., Albert, M., Frank, R., Hsiao, J., Kaye, J., Quinn, J., Lind, B., Carter, R., Dolen, S., Schneider, L.S., Pawluczyk, S., Beccera, M., Teodoro, L., Spann, B.M., Brewer, J., Vanderswag, H., Fleisher, A., Heidebrink, J.L., Lord, J.L., Mason, S.S., Albers, C.S., Knopman, D., Johnson, K., Doody, R.S., Villanueva-Meyer, J., Chowdhury, M., Rountree, S., Dang, M., Stern, Y., Honig, L.S., Bell, K.L., Ances, B., Carroll, M., Leon, S., Mintun, M.A., Schneider, S., Oliver, A., Marson, D., Griffith, R., Clark, D., Geldmacher, D., Brockington, J., Roberson, E., Grossman, H., Mitsis, E., de Toledo-Morrell, L., Shah, R.C., Duara, R., Varon, D., Greig, M.T., Roberts, P., Albert, M., Onyike, C., D'Agostino, D., Kielb, S., Galvin, J.E., Cerbone, B., Michel, C.A., Rusinek, H., de Leon, M.J., Glodzik, L., De Santi, S., Doraiswamy, P.M., Petrella, J.R., Wong, T.Z., Arnold, S.E., Karlawish, J.H., Wolk, D., Smith, C.D., Jicha, G., Hardy, P., Sinha, P., Oates, E., Conrad, G., Lopez, O.L., Oakley, M., Simpson, D.M., Porsteinsson, A.P., Goldstein, B.S., Martin, K., Makino, K.M., Ismail, M.S., Brand, C., Mulnard, R.A., Thai, G., Mc-Adams-Ortiz, C., Womack, K., Mathews, D., Quiceno, M., Diaz-Arrastia, R., King, R., Weiner, M., Martin-Cook, K., DeVous, M., Levey, A.I., Lah, J.J., Cellar, J.S., Burns, J.M., Anderson, H.S., Swerdlow, R.H., Apostolova, L., Tingus, K., Woo, E., Silverman, D.H.S., Lu, P.H., Bartzokis, G., Graff-Radford, N.R., Parfitt, F., Kendall, T., Johnson, H., Farlow, M.R., Hake, A., Matthews, B.R., Herring, S., Hunt, C., van Dyck, C.H., Carson, R.E., MacAvoy, M.G., Chertkow, H., Bergman, H., Hosein, C., Black, S., Stefanovic, B., Caldwell, C., Robin Hsiung, G.-Y., Feldman, H., Mudge, B., Assaly, M., Kertesz, A., Rogers, J., Bernick, C., Munic, D., Kerwin, D., Mesulam, M.-M., Lipowski, K., Wu, C.-K., Johnson, N., Sadowsky, C., Martinez, W., Villena, T., Turner, R.S., Johnson, K., Reynolds, B., Sperling, R.A., Johnson, K.A., Marshall, G., Frey, M., Lane, B., Rosen, A., Tinklenberg, J., Sabbagh, M.N., Belden, C.M., Jacobson, S.A., Sirrel, S.A., Kowall, N., Killiany, R., Budson, A.E., Norbash, A., Johnson, P.L., Allard, J., Lerner, A., Ogrocki, P., Hudson, L., Fletcher, E., Carmichael, O., Olichney, J., DeCarli, C., Kittur, S., Borrie, M., Lee, T.-Y., Bartha, R., Johnson, S., Asthana, S., Carlsson, C.M., Potkin, S.G., Preda, A., Nguyen, D., Tariot, P., Reeder, S., Bates, V., Capote, H., Rainka, M., Scharre, D.W., Kataki, M., Adeli, A., Zimmerman, E.A., Celmins, D., Brown, A.D., Pearlson, G.D., Blank, K., Anderson, K., Santulli, R.B., Kitzmiller, T.J., Schwartz, E.S., Sink, K.M., Williamson, J.D., Garg, P., Watkins, F., Ott, B.R., Querfurth, H., Tremont, G., Salloway, S., Malloy, P., Correia, S., Rosen, H.J., Miller, B.L., Mintzer, J., Spicer, K., Bachman, D., Finger, E., Pasternak, S., Rachinsky, I., Drost, D., Pomara, N., Hernando, R., Sarrael, A., Schultz, S.K., Boles Ponto, L.L., Shim, H., Smith, K.E., Relkin, N., Chaing, G., Raudin, L., Smith, A., Fargher, K., Raj, B.A., Neylan, T., Grafman, J., Davis, M., Morrison, R., Hayes, J., Finley, S., Friedl, K., Fleischman, D., Arfanakis, K., James, O., Massoglia, D., Fruehling, J.J., Harding, S., Peskind, E.R., Petrie, E.C., Li, G., Yesavage, J.A., Taylor, J.L., Furst, A.J., 2016. Basal forebrain degeneration precedes and predicts the cortical spread of Alzheimer's pathology. Nat. Commun. 7, 13249.

Scott, S.A., Mufson, E.J., Weingartner, J.A., Skau, K.A., Crutcher, K.A., 1995. Nerve growth factor in Alzheimer's disease: increased levels throughout the brain coupled with declines in nucleus basalis. J. Neurosci. 15, 6213–6221.

Seiler, M., Schwab, M.E., 1984. Specific retrograde transport of nerve growth factor (NGF) from neocortex to nucleus basalis in the rat. Brain Res. 300, 33–39.

Sobreviela, T., Pagcatipunan, M., Kroin, J.S., Mufson, E.J., 1996. Retrograde transport of brain-derived neurotrophic factor (BDNF) following infusion in neo- and limbic cortex in rat: relationship to BDNF mRNA expressing neurons. J. Comp. Neurol. 375, 417–444.

Sodero, A.O., Weissmann, C., Ledesma, M.D., Dotti, C.G., 2011. Cellular stress from excitatory neurotransmission contributes to cholesterol loss in hippocampal neurons aging in vitro. Neurobiol. Aging 32, 1043–1053.

Sung, K., Maloney, M.T., Yang, J., Wu, C., 2011. A novel method for producing mono-biotinylated, biologically active neurotrophic factors: an essential reagent for single molecule study of axonal transport. J. Neurosci. Methods 200, 121–128.

Teipel, S., Heinsen, H., Amaro, E., Grinberg, L.T., Krause, B., Grothe, M., 2014. Cholinergic basal forebrain atrophy predicts amyloid burden in Alzheimer's disease. Neurobiol. Aging 35, 482–491.

Uday Bhanu, M., Mandraju, R.K., Bhaskar, C., Kondapi, A.K., 2010. Cultured cerebellar granule neurons as an in vitro aging model: topoisomerase IIβ as an additional biomarker in DNA repair and aging. Toxicol. In Vitro 24, 1935–1945.

Villarin, J.M., McCurdy, E.P., Martínez, J.C., Hengst, U., 2016. Local synthesis of dynein cofactors matches retrograde transport to acutely changing demands. Nat. Commun. 7, 13865.

Whitehouse, P.J., Price, D.L., Struble, R.G., Clark, A.W., Coyle, J.T., DeLong, M.R., 1982. Alzheimer's disease and senile dementia: loss of neurons in the basal forebrain. Science 215, 1237–1239.

Williams, B.J., Bimonte-Nelson, H.A., Granholm-Bentley, A.C., 2006. ERK-mediated NGF signaling in the rat septo-hippocampal pathway diminishes with age. Psychopharmacology (Berl) 188, 605–618.

Williams, B., Granholm, A.C., Sambamurti, K., 2007. Age-dependent loss of NGF signaling in the rat basal forebrain is due to disrupted MAPK activation. Neurosci. Lett. 413, 110–114.

Yamashita, N., Joshi, R., Zhang, S., Zhang, Z.Y., Kuruvilla, R., 2017. Phospho-regulation of soma-to-axon transcytosis of neurotrophin receptors. Dev. Cell 42, 626–639.e5.

Ypsilanti, A.R., Girão da Cruz, M.T., Burgess, A., Aubert, I., 2008. The length of hippocampal cholinergic fibers is reduced in the aging brain. Neurobiol. Aging 29, 1666–1679.

Zhao, X., Zhou, Y., Weissmiller, A.M., Pearn, M.L., Mobley, W.C., Wu, C., 2014. Real-time imaging of axonal transport of quantum dot-labeled BDNF in primary neurons. J. Vis. Exp. e51899.